19th Conference on Severe Local Storms
14–18 September 1998
Minneapolis, MN

P3.3 SOME POSSIBLE MECHANISMS FOR TORNADOGENESIS FAILURE IN A SUPERCELL

David O. Blanchard
NOAA/NSSL*
Boulder, CO

Jerry Straka
School of Meteorology
University of Oklahoma
Norman, OK

1. INTRODUCTION

The Verification of Rotation in Tornadoes Experiment (VORTEX; Rasmussen et al. 1994) was conducted in the southern plains of Kansas, Oklahoma, and Texas during the spring months of 1994 and 1995. A primary goal of the program was to collect data using multiple platforms that would then be analyzed to test and possibly refute various tornadogenesis hypotheses. On June 8, 1995, VORTEX scientists were able to collect data on a strong, long-lived non-tornadic supercell which persisted for many hours and moved from the northeast Texas Panhandle into the Oklahoma Panhandle. The analysis of this storm is presented as an example of tornadogenesis failure.

Doppler radar data from the airborne NCAR Electra Doppler Radar (ELDORA) and the ground-based Doppler on Wheels (DOW), along with the surface mobile mesonet (MM) and mobile sounding systems (M-CLASS) were used to collect data while near and underneath the storm. The high spatial and temporal resolution of these data allow for a detailed analysis of the three-dimensional wind field of the storm. Comparison between this non-tornadic supercell storm and other tornadic storms sampled in VORTEX clearly illustrate that many of the relevant features to the tornadogenesis process are also present in this storm. An analysis of the dominant circulation features, the evolution of the rear and forward flank downdrafts, the cyclonic/ anticyclonic circulation couplets, surface boundaries, and other features of the storm will attempt to determine the possible causes of tornadogenesis failure.

2. DATA

VORTEX scientists were able to collect multisensor data sets of this nontornadic supercell as it traversed Beaver County, Oklahoma, on June 8, 1995. Airborne Doppler radar data is available from ELDORA starting at 1950 UTC; the aircraft completed 17 pseudo-Doppler legs between 1950 and 2150 UTC. The most interesting data is restricted to the period 1950–2045 UTC. DOW data collection started a few minutes later; 21 volume scans are available from 1958–2042 UTC. Surface data is available from the MM; multiple vehicles with pressure, temperature, relative humidity and wind sensors were near and underneath the storm during the period of time that Doppler radar data was collected. Rawinsonde data are available from multiple M-CLASS soundings that were launched in northwestern Oklahoma.

3. WHAT IS TORNADOGENESIS FAILURE?

The vast majority of thunderstorms do not produce tornadoes. Even most supercells do not produce tornadoes (Rasmussen 1998a; Burgess 1998, personal communication). So what makes this event an example of "tornadogenesis failure?" And when did "tornadogenesis failure" occur (Trapp 1998)? It's easy to construct a time line for a tornadic event with pre-tornadic, development, mature, and dissipation stages. How do we do the equivalent for a non-tornadic storm? Stated differently, *What didn't happen? And when did it not happen?*

4. LARGE-SCALE SETTING

A quasi-stationary frontal boundary was oriented NNE–SSW across the eastern Oklahoma Panhandle and into the northern Texas Panhandle. The Beaver County storm was the first supercell of the day, initially developed near or on this frontal boundary at ~1845 UTC, and then moved slowly northeast at a speed of ~4 m s^{-1} during its supercell phase. Additional storms that became tornadic supercells formed shortly thereafter (~1915 UTC) along the dryline in the central portions of the Texas panhandle. Approximately 1 h later (1955 UTC) both the Amarillo, Texas (AMA), and Dodge City, Kansas (DDC), WSR-88D Doppler radars indicated a supercell with a hook echo and mesoscyclone in Beaver County, Oklahoma.

Satellite imagery and animations indicate that there was an extensive region of low stratus located a few tens of kilometers north of the frontal zone. During the morning, numerous waves were observed to propagate south of the boundary into the stable boundary layer of the warm sector. Other boundaries were also detected in the warm sector. By early afternoon, there was a well-defined line of cumulus clouds associated with the front.

* Additional affiliation: CIMMS/University of Oklahoma, Norman, OK.

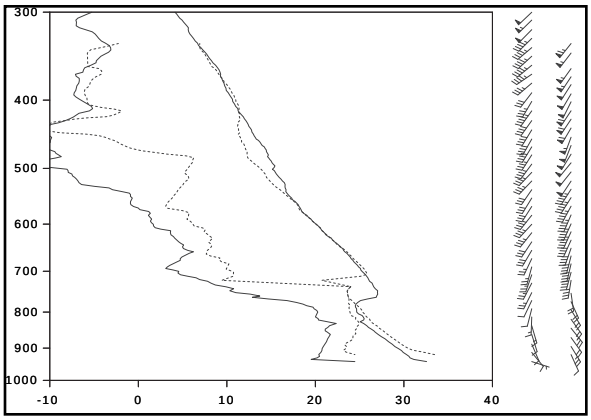

Figure 1. Skew T–log P diagram of soundings taken in northwestern Oklahoma. Profiles are at 1830 UTC (solid lines, wind barbs on left), and 2030 UTC (dashed lines; wind barbs on right).

5. ANALYSIS OF THE STORM

Rawinsonde data are available from multiple M-CLASS soundings that were deployed in northwestern Oklahoma. The first launch was at ~1800 UTC (Fig. 1) and indicated strong shear and large instability. A second rawinsonde was launched nearby at ~2030 UTC and indicated that the base of the elevated mixed layer (EML) lifted from ~750 to 700 mb. There was also considerable moistening of the boundary layer during this period. Lifted surface parcels reached saturation below the EML and continued to ascend past the inversion but with reduced accelerations. Once the parcel had ascended above the base of the EML, the parcel likely experienced tremendous accelerations. Thus, although there was large total CAPE (in excess of 4500 J kg^{-1}), there was very little low-level CAPE, and NCAPE in the lowest few kilometers was small (Blanchard 1998). This may have been a contributing factor to tornadogenesis failure.

1950 UTC: The first volume scan from ELDORA shows a well-defined hook echo (Fig. 2) at 2000 m MSL (~1300 m AGL). There is a velocity couplet, located near the tip of the appendage, with 30 m s^{-1} shear across the circulation and 25 m s^{-1} gate-to-gate shear. Further aloft (4000 m MSL), the velocity couplet exceeds 55 m s^{-1}, although the gate-to-gate shear is only 10 m s^{-1}, indicative of a well-developed, but unfocused mesocyclone. Pseudo-RHI (range-height indicator) scans from the aircraft show the weak echo region (WER) and precipitation loading aloft, suggesting strong updraft speeds are present. Objective analysis of the data shows that the vertical component of vorticity is elongated with a northeast–southwest orientation (Fig. 3). This configuration was observed during many of the subsequent volume scans.

1958 UTC: At both 1500 and 2500 m MSL, there is a thin hook echo evident (Fig. 4) with an elongated forward flank region. A new circulation center is located southwest of the original center and exhibits ~25 m s^{-1} shear. The appendage exhibits both a cyclonic and anticyclonic hook, a feature noted in many tornadic supercells. At 8500 m MSL (not shown), a large, hook-shaped echo is present and there is >40 m s^{-1} shear present although the gate-to-gate shear is weak. A pseudo-RHI through the hook region shows that the WER has become more pronounced. Downward velocities are in excess of 65 m s^{-1} in the anvil region adjacent to the strong updraft, and a horizontal vortex roll is evident in both the reflectivity and velocity data.

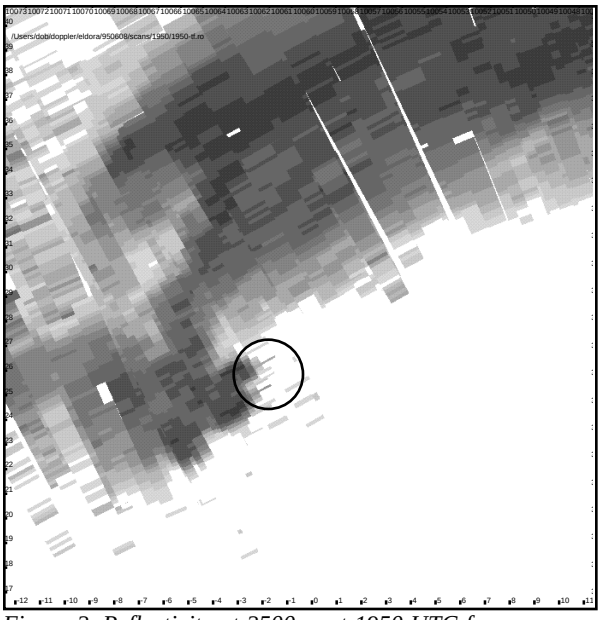

Figure 2. Reflectivity at 2500 m at 1950 UTC from ELDORA. Strongest values in the forward flank region are about 50 dBz. Darker gray shades correspond to higher dBz values. The circle denotes the region containing the velocity couplet.

2004 UTC: At 2500 m MSL, the arm of the hook is extended NNE–SSW. Velocities in this region show ~22 m s^{-1} shear (–18/+4 m s^{-1}). Further aloft at 5000 m, a clear slot is visible in the reflectivity and is likely associated with the developing rear flank downdraft (RFD). A pseudo-RHI through the hook shows that the WER now extends up to ~12 km. The vertical vorticity maximum is aligned NE–SW with strongest values (~0.05 s^{-1}) located northeast of the tip of the hook. A weak secondary maximum is located on the southwest end of the hook. At 14000 m MSL, a semicircular region of downdraft (Fig. 5) is located upshear and cross shear of the overshooting top. This downdraft extends from this level all the way down to the lowest analyzed levels.

2012 UTC: At 2000 m MSL, the hook has continued to become more extruded and lengthen and narrow. The velocity couplet is –18/+4 m s^{-1}, although the true

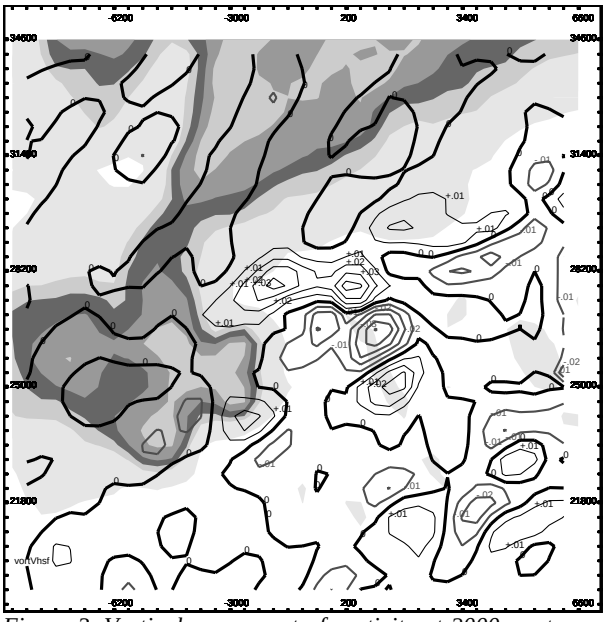

Figure 3. Vertical component of vorticity at 2000 m at 1950 UTC from ELDORA. Contours are every 2x10^{-2} s^{-1}; positive values are think black lines, negative values are thick gray lines. Gray shading denotes the storm reflectivity with darker shades corresponding to higher dBz values.

strength of the couplet may be too small to detect reliably. This scale contraction was also noted in the Dimmitt, Texas, tornadic storm of June 2, 1995 (Rasmussen 1998b). An RHI shows that the WER now extends to 16 km. Downward vertical velocities of >75 m s^{-1} are noted adjacent to the overshooting convective updraft. A cyclonic/anticyclonic vorticity couplet is present at this time and the vorticity at lower levels (1500–2400 m) is still elongated in a northeast–southwest orientation.

2016 UTC: At this time, VORTEX crews reported a small, brief funnel cloud. At 2500 m MSL, a hook echo is still clearly evident, as are two distinct circulation centers. The circulation associated with the southwestern vorticity center appears to be associated with rapidly growing cumulus and a new mesocyclone; the circulation associated with the northern circulation center is still associated with the strong updraft. DOW radar data at this time clearly shows a tornado-like signature in the reflectivity and velocity fields (Fig. 6). Velocities at the base tilt (~80 m AGL) show a velocity couplet with 20 m s^{-1} shear, yet this circulation did not produce a visible cloud swirl on the ground, based on reports from the numerous VORTEX crews operating in the area. Unlike the Dimmitt, Texas, supercell, no spiraling band of anticyclonic vorticity adjacent to the hook is noted.

2020–2036 UTC: During this period, the DOW continued to show two circulations centers: one was located near the tip of the hook echo; the other circulation was

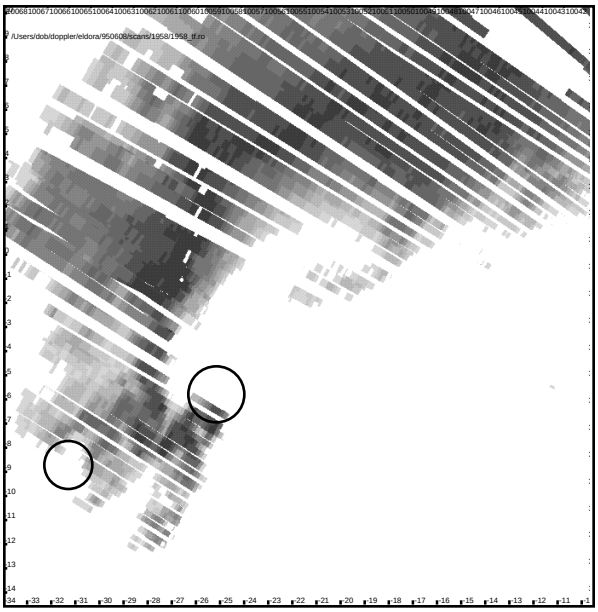

Figure 4. As in Fig. 2 except for 2500 m at 1958 UTC.

located farther to the southwest and was associated with the RFD. This velocity couplet was ~20–30 m s^{-1} and was observable at the lowest tilt so that the circulation was present at ~80 m AGL. Yet no circulation was noted on the ground by the MM or by the presence of lofted dust or other debris. MM observations suggest that an extremely shallow layer of cool outflow air underlay this circulation preventing contact of the circulation with the ground. Clearly this weak tornadic circulation aloft was “almost” a tornado, so the question is asked, “When is a tornadic circulation not a tornado?”

6. SUMMARY

The preliminary analysis of this non-tornadic supercell indicates that VORTEX teams and data platforms arrived "in time" for documentation of this storm. Many features noted in this non-tornadic storm were also seen in the Dimmitt, Texas, (2 June 1995) tornadic storm. Comparisons between these two storms indicates that the difference between a tornadic supercell and a non-tornadic supercell may be exceedingly subtle as our observations improve and we probe deeper into the cloud-scale circulations of supercells. The Elmwood, Oklahoma storm of 8 June 1995 certainly fits the classifications of a “tornadogenesis failure."

The presence of a layer in the lower troposphere with only weak buoyant instability may present a situation in which accelerations near cloud base are insufficient to effectively spinup vertical vorticity through stretching. or to tilt horizontal vorticity into the vertical. This would indicate that strong buoyant instability at and above the LCL and LFC might be important features for the development of the low-level mesocyclone and tornado. The RFD was well developed as indicated

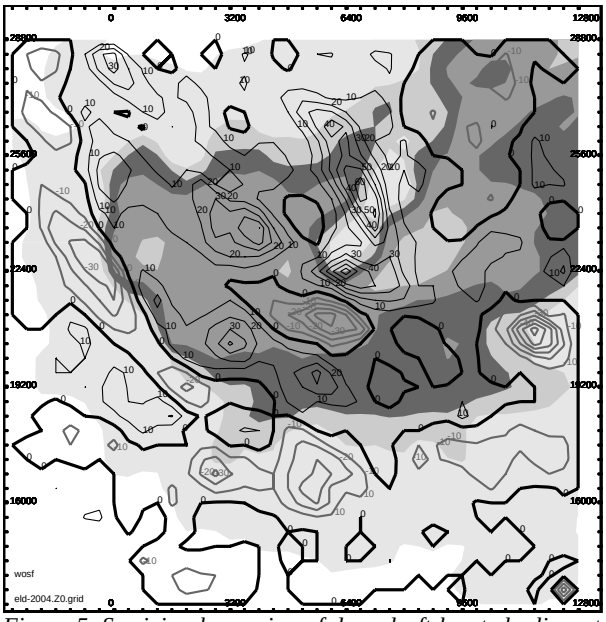

Figure 5. Semicircular region of downdraft located adjacent to the high reflectivity region associated with the updraft. The contour interval is 10 m s–1; positive values are thin black lines, negative values are thick gray lines.

by the region of strong downdraft on the upshear side of the storm and extended from near the anvil level down to the lowest analyzed levels. Data from the mobile mesonets suggest that the leading edge of the RFD and gust front may have surged out slightly ahead of the main updraft. This surge was very shallow and was not detected by either the airborne ELDORA or the DOW, even though the latter was only a few kilometers away from the circulation and was scanning at less than one hundred meters above the ground. This result suggests that the operational WSR-88D radars may not be able to distinguish between supercells with a surging RFD and gust front and those where the gust front remains under the main updraft unless the storm is extremely close to the radar.

Recent work has suggested that a thermodynamic retrieval analysis can improve our understanding of the dynamic processes leading to tornadogenesis or tornadogenesis failure. We have not attempted to do a thermodynamic retrieval on this event for at least two reasons. The National Weather Service has no capability to do this in real time when the issuance of timely warnings is critical. One of our goals is to provide information that can be used in this "short-fuse situation" to aid in the dissemination of appropriate warnings. Another reason is that the evolution of processes responsible for the tornado occur on very small time and space scales. These scales may violate the assumptions often used when computing the three-dimensional wind field from radial wind components and subsequently places doubt on the accuracy of such a retrieval.

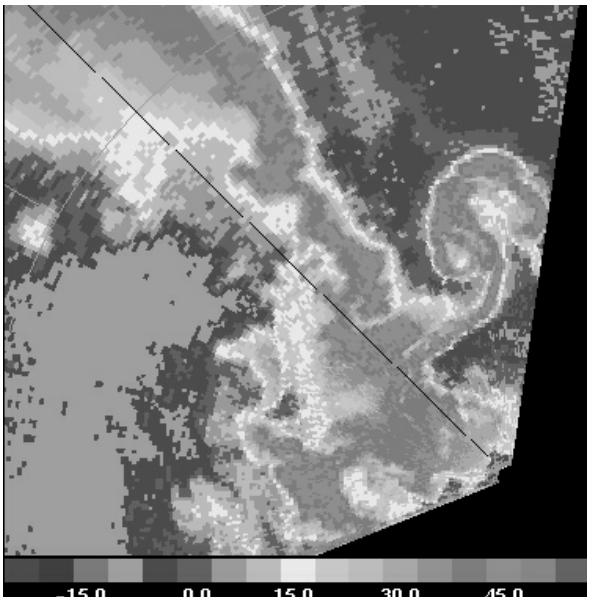

Figure 6. Base tilt of radar reflectivity depicting a velocity couplet and "eye" at 3 km and ~80 m altitude. Radar data is from the DOW mobile platform.

Finally, interested readers are invited to browse the VORTEX web pages for an extended version of this case study at <http://mrd3.mmm.ucar.edu/~vortex/www/950608/elmwood-db.html>.

Acknowledgments: The authors would like to extend their appreciation to the joint efforts of NCAR, NSSL, and OU for the development and deployment of the Doppler on Wheels. Portions of this research were supported by National Science Foundation grant numbers ATM-9617318 and ATM-9120009.

REFERENCES

Blanchard, D. O., 1998: Assessing the vertical distribution of convective available potential energy. *Wea. Forecasting*. (In press.)

Rasmussen, E. N., J. M. Straka, R. P. Davies-Jones, C. A. Doswell, F. Carr, M. Eilts, and D. R. MacGorman, 1994: Verification of the origins of rotation in tornadoes experiment: VORTEX. *Bull. Amer. Met. Soc*, **75**, 995–1006.

Rasmussen, E. N., 1998a: A baseline climatology of sounding-derived supercell and tornado forecasting parameters. *Mon. Wea. Rev.* (Accepted).

Rasmussen, E. N. cited 1998b: Recent findings from VORTEX. [Available on-line from http://mrd3.mmm.ucar.edu/~eras/www/MyPage/Talks/st98/WWW.html.]

Trapp, R. J., 1998: Observations of nontornadic low-level mesocyclones and attendant tornadogenesis failure during VORTEX. *Mon. Wea. Rev.* (Accepted).